Seismic Assessment of Masonry Arch Bridges

Luca Pelà [1*], Alessandra Aprile [1], Andrea Benedetti [2]

[1] *ENDIF Department , University of Ferrara, Italy*

[2] *DISTART Department , University of Bologna, Italy*

Abstract

In this paper, the seismic performance of existing masonry arch bridges is evaluated by using nonlinear static analysis, as suggested by several modern standards such as UNI ENV 1998-1 2003, OPCM 3274 2004, FEMA 440 2005. The use of inelastic pushover analysis and response spectrum approaches, becomes more difficult when structures other than the framed ones are investigated. This paper delves into the application of this methodology to masonry arch bridges by presenting two particular case studies. The need for experimental tests in order to calibrate the materials and the dynamic properties of the bridge is highlighted, in order to correctly model the most critical regions of the structure. The choice of the control node in the pushover analysis of masonry arch bridges and its influence on seismic safety evaluation is investigated. The ensuing discussion emphasizes important results, such as the unsuitability of the typical top node of the structure for describing the bridge seismic capacity. Finally, the seismic safety of the two bridges under consideration is verified by presenting an in depth vulnerability analysis.

Keywords: masonry arch bridges; non-linear analysis; pushover analysis; displacement-based design; performance based seismic design; seismic assessment of existing bridges; control node; energy-based pushover analysis; energy equivalent displacement.

[*] Corresponding author: Luca Pelà

ENDIF Department, University of Ferrara, Via Saragat 1, 44100 Ferrara, Italy

Tel: +39 0532 974943 Fax: +39 0532 974870 email: luca.pela@unife.it

1. Introduction

Unreinforced masonry structures are found in many earthquake-prone countries. Nowadays, particular attention is paid to existing masonry arch bridges because of their great importance for national road and rail networks. In fact, the majority of the bridges in the European railway network, as well as a large part of those in the road system consist of masonry structures. Therefore, their assessment is strongly needed by railway and local administrative authorities.

In the last 25 years, several procedures were developed in order to predict the behaviour of masonry arch bridges. The difficulty in representing the behaviour of the material and the resistant skeleton requires the use of a simplified but effective structural model. The developed methodologies, which could be based on Limit Analysis [1-4] and non linear incremental techniques [5-7], usually refer to bi-dimensional arches. Improved bi-dimensional models, which take into account the arch-fill interaction, were also developed [8-11]. In addition, three-dimensional FEM models [12,13] allow both a complete description of the bridge geometry and detailed constitutive models. Unfortunately, only a few studies available today concern themselves with the seismic assessment of masonry bridges [14].

Structural analysis in earthquake engineering is an involved task, because the activated structural behaviour is typically nonlinear, the structural system is usually complex, and the input data (structural properties and ground motions) are random and uncertain.

In principle, the nonlinear time-history analysis is the most suitable seismic evaluation tool, but such an approach cannot be considered common practice yet. Moreover, dynamic nonlinear analysis is strongly dependent on the input parameters' uncertainty and has a high computational cost, which must be considered when complex structures are analysed.

The methods suggested by the great majority of the codes dealing with existing buildings are based on the assumption of linear elastic structural behaviour and do not provide information about real strength, ductility and energy dissipation. They also fail to predict the expected damage in quantitative terms.

At the moment, the most rational analysis methods for practical applications seem to be the simplified inelastic analysis procedure, which combines the non-linear static (*pushover*) analysis and the response spectrum approaches. Procedures derived from this method have been recently introduced in several modern codes [15-19], in which great attention is given to the new *performance-based design* philosophy.

In this paper, the analyses of two real case studies are worked out in detail in order to highlight the performance of different safety evaluation formats.

The results obtained point to the need for a careful characterization of the material, since the variability of the mechanical parameters describing the masonry behaviour heavily influences the results of the nonlinear static analysis.

In conclusion the present work reveals that the choice of the control node position in the pushover analysis can modify in a significant way the slope of the capacity curve, but that its influence in the safety margin evaluation is not so great. Although for the examined cases the centre of mass appears to be the best compromise choice, further analyses are needed to confirm this result.

2. Geometrical Data and Materials

The bridges considered in this paper (fig. 1) are situated about 30 km northwest of *Pistoia* (Italy), in two villages called *S. Marcello Pistoiese* and *Cutigliano,* respectively. They are both triplearched stone bridges, built after the 2nd World War to cross the *Lima* river in the Tuscany region. The first one has brick-made vaults, while the second one has concrete-made vaults. Sandstone blocks from the rocks of the surroundings were adopted for the constructions. Lime mortar was used for the deeper parts of the bridges; concrete mortar was used for all visible surfaces and for the bricks of the first bridge vaults.

The foundations of the piers are of a high load bearing capacity rocks by means of reinforced concrete footings. The waste material obtained from excavation of the foundations constitutes the fill above the vaults and between upstream and downstream spandrel walls.

The main geometrical data of the bridges are summarized in Tables 1 and 2; more information is given by figs. 2 and 3.

3. Identification and Modelling of Material Properties

Material properties were assessed according to laboratory and field testing results. Seven stone cores were drilled from the bridges and were subjected either to compression and splitting tests (fig. 4), in order to evaluate the stone elastic modulus and the compressive and tensile strength. The laboratory tests results (Table 3) showed the good mechanical properties of the stone elements. The scatter of test results of different specimens is considerable, for the particular case of the compressive strength. This fact is due to the material heterogeneity and to the different conditions of degradation of the extracted stones. In the case of masonry, it is quite typical to obtain a large dispersion of data both for artificial and natural blocks [3, 23]. In the case of natural elements, the sedimentation geometry of the quarry is the factor of greatest influence; in the case of artificial ones, clay composition and oven temperature give rise to the observed statistical variations.

The assessment of the characteristic strength of the existing mortar was carried out by way of the penetrometric mechanical in-situ test [20]; the results provided a characteristic strength of about 0.3 MPa.

Furthermore, the bridges were subjected to on-site non-destructive tests, based on the dynamic response analysis to impelling force. Such an experimental approach allows for the identification of the principal dynamic characteristics of the structure, in order to set the mechanical parameters and the restraint conditions of the numerical model. An impelling force was transversally applied to each bridge next to the middle arch crown. In this position, an accelerometer was placed in order to record the consequent horizontal acceleration values (figs. 2-a and 3-a).

For sake of data identification, 3-D finite element models were worked out using eight or six node brick solid elements. The FEM code Straus7 [21] was used for the analysis; this software is typically used by designers and professionals for structural analysis. Masonry was modelled as a homogeneous material so that average response properties are considered.

The comparison between experimental and numerical results in terms of vibration frequencies and modal shapes allowed for the calibration of the mechanical parameters and the restraint conditions of the finite element model [22]. Figs. 5 and 6 show the acceleration signals recorded in the proximity of the middle arch crown (a), with the respective power spectral density (b) and modal shape numerically determined (c).

In the case of the S. Marcello Pistoiese bridge, the impelling force applied at the middle arch crown excites only the mode with frequency equal to about 4 Hz (fig. 5-b), which is the first mode in the transversal direction of the bridge (fig. 5-c).

Fig. 6-b shows the natural frequency spectrum of the Cutigliano Bridge. In this case, the impelling force excites the modes with natural frequency equal to about 6 Hz and 23 Hz. The Cutigliano bridge is stiffer than the S. Marcello one because it has concrete-made vaults. It is also important to remember that the Cutigliano Bridge is not symmetrical. Fig. 6-c shows the modal shape 4, correspondent to a frequency equal to 23.1 Hz.

By considering the laboratory and dynamic tests, the values of the mechanical structural parameters to be adopted in the numerical models were selected (Table 4). In particular, in the analysis all the materials secant Young's moduli were set equal to one half of the determined dynamic ones [23].

Since only two mechanical parameters were extracted from the tests, a two parameter model is sufficient for the description of the material's behaviour. A Drucker-Prager model with pressure sensitive elastic-plastic material, with associated flow rule and isotropic behaviour, is thus selected to represent the materials (masonry, concrete, backfill) of the bridges.

The non-linear analyses were performed making use of the Drucker-Prager failure criterion since it brings considerable advantages from the analytical and computational point of view due to its smooth failure surface. This two-parameter model permits us to express the friction angle ϕ and the cohesion c in terms of the uniaxial tensile strength f_t and the compressive strength f_c [24] explicitly. The parameter values were computed for each different tested material and implemented in the numerical models.

For the backfill, we assumed ϕ = 20°, c = 0.05 MPa, while for bricks and concrete mortar masonry ϕ = 55°, c = 0.05 MPa; these values were chosen as those suggested by Italian guidelines [17] and following engineering judgement. The concrete of the Cutigliano bridge vault was characterized by ϕ = 55° and c = 1.15 MPa.

Concerning the sandstone blocks masonry, which constitutes the major part of the bridge structure, no significant specimen could be extracted and tested; furthermore, the usual homogenization formulas are not useful for random textured masonry. Therefore, a parametric study was performed as a risk assessment tool in order to consider the strength parameters f_t and f_c as average properties of the homogeneous continuum representing the behaviour of the masonry composite material.

In particular, since the range of strength ratios in masonry compounds is limited, the masonry tensile strength f_t and the ratio f_t/f_c between masonry tensile and compressive strength were selected as the main variables of the investigation.

The Drucker-Prager's constants of the stone masonry considered for the analysis were computed for different values of f_t (0.2, 0.3 and 0.4 MPa) and f_t/f_c (1/10, 1/15 and 1/20), chosen on the basis of common experience. The obtained parameter values are reported in Table 5.

The soil reaction at the pier footing was modelled with particular elements, called *cut-off bars*, which properly account for the plastic behaviour of these critical sections. Cut-off bars present an elastic-plastic constitutive law, with different yielding strength in traction and compression. These elements are defined by fixing axial stiffness and cut-off values (maximum permissible tension and compression forces), so that they can simulate the soil reaction beneath the plinth. This expedient permits us to localize the damage at the pier end for a better numerical control when the limit state of overturning is about to be approached.

4. Pushover Analysis

In recent years, displacement-based methodologies such as the pushover analysis have been proven to be consistent in the seismic evaluation of existing buildings. In recent codes [15-18], the use of such non linear methods has been extended to the case of unreinforced masonry buildings.

In this article, an application of this tool is studied for the particular case of masonry arch bridges. Recent studies on this structural typology showed that the simplified method, under the usual restricting hypotheses of the pushover analysis, slightly overestimate in a conservative way the displacement obtained by nonlinear dynamic direct integrations [14].

Standard pushover analysis may not detect the structural weaknesses, which are generated when the structure dynamic characteristics change after the formation of the first local plastic mechanism [25,26]. The adaptive pushover analysis [27] allows us to account for the reduction in the structural stiffness which occurs during the earthquake, but requires more computational effort and its application to masonry structures is not straightforward. The document FEMA 440 [18] presents an in-depth review of the research on nonlinear static seismic analysis procedures.

For the masonry bridges under consideration here, a preliminary natural frequency analysis was carried out in order to determine the bridges' resonant frequencies and the mode shapes. These analyses showed the prevailing influence of the first mode of vibration on the dynamic behaviour of the structures. Since the first mode shape occurs in the transversal direction (Z), the most critical failure mechanism takes place for forces acting orthogonal to the plane containing the pier axes.

Pushover analyses were performed by applying to each bridge a monotonically increasing pattern of transversal forces, representing the inertial forces which would be experienced by the structure during the ground shaking.

The loading is imposed in a two-step sequence making use of a numerical model characterized by material and geometric non-linearity. In the first step, the vertical (permanent) load is applied and in the subsequent steps the lateral loads are added in an incremental way. The maximum capacity of the structure corresponds to the situation in which a further lateral load increment is impossible. In particular, such a force-controlled loading does not allow for a detection of the softening branch of the response. The more appropriate displacement-controlled procedures are not always permitted by the common commercial finite element programs.

The selection of an appropriate lateral load distribution is a key factor of the pushover analysis, since the loads should represent the inertial forces acting on the structure during the earthquake. In the present work, lateral forces proportional to the mass distribution are used.

The capacity of the structure is described by the curve of the base shear force versus the displacement at a suitable control point. Therefore, a complex structural behaviour is converted into the response of an equivalent nonlinear single degree of freedom system (SDOF), permitting a direct comparison with the seismic demand in terms of the response spectrum.

The rules for the conversion however, are still in debate. A discussion on the selection of the control node will be postponed until section 6.

Figure 7 shows the effectiveness of the static non linear method in pointing out the parameter sensitivity of the model, with relation to the compressive and tensile strength of the masonry material. Figures 7-a and 7-b represent the effect of both the above-mentioned parameters on the seismic capacity of the San Marcello Pistoiese bridge. The set of these curves is obtained by posing the centre of the mass of the structure as control point. In section 6, other choices will be presented, discussed and compared.

5. Seismic Performance Analysis: Theoretical Background

The seismic performance evaluation is carried out by making use of the N2 method, as developed by *Fajfar* [25,26]. Today this procedure is reported by several modern codes, like Eurocode 8 [15] and the New Seismic Italian Code [16,17]. The N2 method is an advancement with respect to of the *Freeman*'s "Capacity Spectrum method" [28,29], further applied in FEMA 356 [19] and FEMA 440 [18].

The method presented in this work is formulated in the acceleration-displacement (AD) format. Following this approach, the capacity of the structure is directly compared with the demand of the earthquake ground motion on the structure. The selected format makes possible a graphical interpretation of the procedure and explicates the relationships among the basic parameters controlling the seismic response.

The capacity of the structure is represented by a global force-displacement curve, obtained as reported in Section 4. The base shear forces and displacements are respectively converted into spectral accelerations and spectral displacements of an equivalent SDOF system. These spectral values allow drawing the capacity diagram.

With regard to the seismic demand, the elastic spectra reported in the codes [15-17] were converted into inelastic spectra with constant ductility, using simplified relations given by *Vidic et al.* [30] in terms of the ductility factor μ and the ductility dependent reduction factor R_μ (see also [31]).

The inelastic demand in terms of accelerations and displacements is given by the intersection point of the capacity diagram with the demand spectrum corresponding to the ductility demand μ. In this point, called *performance point*, the ductility factor determined on the capacity diagram must be equal to the value associated with the intersecting demand spectrum.

Recently, the N2 method has been proposed for the seismic analysis of masonry structures; many works found in the literature concerning masonry buildings [31] and arch bridges [14] explain the effectiveness of this procedure for these peculiar construction classes. Furthermore, recent studies on bridges similar to the ones studied in this work show that the simplified method slightly overestimates in a conservative way the displacement obtained by nonlinear dynamic analysis; this trend is monotonic and proportional to the increase of the earthquake peak ground acceleration [14].

This topic however is still debated in the literature and many researchers are actually working to obtain comparisons by means of advanced dynamic nonlinear analyses.

With the aim of gathering experimental evidence, the authors have recently started an experimental laboratory investigation on scaled masonry bridge models.

6. Choice of the Control Node in the Pushover Analysis

The choice of the control point best suited for outlining the building capacity curve is a complex task, strongly connected to the selection of the structure equivalent SDOF system. Several suggestions were proposed for concrete [32] and masonry [31] buildings, but in the particular case of arch bridges the equivalence is not straightforward.

The N2 method recommends choosing the control point at the roof level and such an instruction seems coherent and logical, because it permits control of a node that certainly is situated above the level where the failure mechanism occurs.

Moreover, recent studies [33,34] use a displacement value computed from the work done in the pushover analysis to establish the capacity curve, in contrast to the use of the roof displacement adopted in conventional procedures. Such an energy-based approach allows one to avoid the errors of the SDOF system capacity curve due to significantly higher modes in the MDOF system, when disproportionate increases and even outright reversals in the roof displacement occur.

For masonry historical buildings, an exhaustive theoretical study is not available and thus, according with the N2 method, the control node is usually assumed to be on the top of the structure. For the sake of argument, some works concerning the pushover analysis of a typical three-nave bay of gothic cathedrals [35,36] can be mentioned. In these studies, the point is considered to be at the top of the central nave.

Referring to the particular case of masonry arch bridges, some authors defined the capacity curve considering the displacement of a node situated at the same height of the seismic forces gyration centre [14]. If the lateral loads are set proportional to the mass distribution, the point clearly will be located at the bridge's centre of mass.

In the present work, the influence of the control node position on the seismic safety evaluation has been checked by using different selection rules. In this comparison, the numerical model of the S. Marcello Pistoiese bridge was considered; the masonry compressive strength f_c was assumed to be equal to 4.5 MPa and the tensile strength f_t equal to 0.3 MPa.

In the pushover analyses, three different control node positions were investigated. Two positions are real, situated respectively at the middle span of the bridge deck and at the centre of mass (at an elevation of 15.8 m, see fig. 2).

The third position is virtual and calculated by means of the Energy Approach [37,38]. Since the structural inelastic behaviour of the MDOF system is essentially governed by energy concepts, the Energy Approach defines a suitable virtual energy equivalent displacement. The energy equivalent displacement can be used to estimate a SDOF capacity curve, which reproduces the total elastic and plastic energy accumulated by the whole structure (MDOF system) during the pushing procedure. The energy equivalent displacement does not correspond to a particular point of the MDOF model, but it is the virtual value which equals the energy capacities of both models. When the Energy Approach procedure is applied, the area of the capacity curve of the SDOF system reproduces exactly the deformation energy of the MDOF system [37,38].

Figure 8 shows the three capacity curves obtained by making reference to the top of the structure displacement (TOP), the centre of mass displacement (CM) and the virtual energy equivalent displacement (EN). As can be easily seen, the energy equivalent displacement yields the stiffest capacity curve, while the top displacement obviously provides the highest values on the x-axis, since it is the maximum displacement of the bridge at every step of the analysis.

The ultimate displacements were determined for each case mentioned and called, respectively, $d_{u,TOP}$, $d_{u,CM}$, $d_{u,EN}$: the corresponding obtained values were 0.125 m, 0.065 m and 0.044 m. The performance point displacements $d_{p,TOP}$, $d_{p,CM}$, $d_{p,EN}$ were also defined by comparing the capacity curves with the demands resulting from the ground motions defined by Italian Seismic Code [16,17]. Several seismic classes were investigated: the 1st , the 2nd and the 3rd, respectively, associated with a ground acceleration value of a_g equal to 0.35 g, 0.25 g and 0.15 g. Two ground amplification factors were considered equal to 1 and 1.25; they refer respectively to ground types A (rock or other rock-like geological formations) and B (deposits of very dense sand, gravel, or very stiff clay).

The obtained results are summarized in Table 6, where the safety factors d_u/d_p are also indicated. The same table reports also the comparison with the ultimate displacements $d_{u,N2}$ obtained by means of the rigorous procedure suggested by the N2 method [25,26]. The means and the coefficients of variation (C.O.V.) of the 4 different safety factors calculated for each seismic demand are also indicated.

Figure 9 shows the graphical comparison between the safety factors d_u/d_p, which are determined considering the top displacement, the centre of mass displacement, the virtual energy equivalent displacement and the N2 displacement. The respective values $(d_u/d_p)_{TOP}$, $(d_u/d_p)_{CM}$, $(d_u/d_p)_{EN}$, $(d_u/d_p)_{N2}$, are referred to pertinent demand spectra.

As can be easily seen, the choice of the top displacement always leads to the highest estimate of the safety factor. The usual choice of this particular node in the pushover analyses [35,36] does not seem suitable, because it implies a more flexible structure, which could be supported only by accounting for higher damping values.

The determination of the N2 displacement is quite time-consuming for a mass-distributed structure and the procedure seems conceptually more adequate to the case of framed structures where the masses could be considered lumped at the storeys.

Intuitively, the choice of the centre of mass or the choice of the energy equivalent displacement permit one to study the response of more representative points. In fact, the virtual energy equivalent displacement is related to an energy-equivalent SDOF system with a height length less than the elevation of the centre of mass (see fig. 8). Since the centre of mass is located above the pier top, it is possible to conclude that these two nodes could be considered relevant for such type of bridges, for which the drift of the piers dominates the out of plane collapse displacement shape, in a manner similar to a cantilever column.

By comparing the aforementioned process with the other two approaches, the choice of the centre of mass or the choice of the energy equivalent displacement lead to lower estimates of the safety factor. Figure 9 also shows that the values of $(d_u/d_p)_{CM}$ and $(d_u/d_p)_{EN}$ come out quite similar even when different seismic demand levels are considered. In any case, the energy equivalent displacement always provides the lowest estimate of the safety factor.

For an assigned probabilistic distribution of the seismic demand, the rigorous probabilistic definition of the bridge seismic safety should require the determination of the probabilistic distribution of the safety factor values by varying the selection of the control node in the pushover analyses. A suitable ideal procedure could consider the probabilistic distribution of the safety factors d_u/d_p corresponding to a regular grid of several control points, but such a procedure could be very time-consuming and there is no proof that the optimum point can be found. However, in the present work, the small set of control points adopted leads to a moderate variability of the results, despite the fact that they are located at different elevations. This fact can be easily noticed in Table 6, where the coefficients of variation appear small. Since the estimate of the safety factor that provides the maximum safety margin should be the minimum of the ones investigated, i.e. the safety factor related to the energy displacement, in the next section the centre of mass displacement will be preferred to assess seismic safety. In fact, the choice of the centre of mass of the bridge is very near to the energy equivalent results, but has a clearer geometrical interpretation and requires less computational effort.

7. Seismic Performance Analysis Results

The bridges analysed herein are situated in the 3rd category seismic zone, with ground acceleration peak value $a_g = 0.15\ g$, as derived by the classification maps of the Italian Seismic Code [16].

However, these bridge structures are particularly diffuse in Italy and the obtained results can be easily generalized and applied to other similar masonry arch bridges. Therefore, the structural capacity was compared with the demand of earthquake ground motions related to 1st, 2nd and 3rd category seismic zones and with reference to ground types A and B.

In figures 10 and 11 the graphical representation of the executed study is reported for both the cases of the Cutigliano and the S. Marcello Pistoiese bridges. A bilinear elastoplastic idealization of the capacity curves based on the equal energy principle was applied in order to determine the performance points, according to references [15-19,25,26,37,38]. Therefore, the procedure could be better worked out by means of the design spectra defined by assigned ductility. Furthermore, the correlation between the capacity curve and its bilinear elastoplastic idealization, which is expressed in terms of the deformation energy and the ductility ratio, assumes an actual significance.

The bridges displacement capacity results were generally higher than the seismic demand; the only exception was found in the S. Marcello Pistoiese Bridge with a 1st category spectrum, ground type B and poor masonry characteristics (see table 7). However, the strength of both structures is quite good on the average. For a large subset of seismic demands, the bridges performance points are located in the elastic branch of the capacity curve, especially for masonry of good quality or concrete vaults as in the case of the Cutigliano bridge.

The obtained results show how this method permits one to consider explicitly the fundamental role of displacement, which is the real effect of the earthquake on the structure. Making reference to the *Displacement Based Design* philosophy, a synthetic check was carried out by comparing the structural displacement capacity, obtained from the pushover analysis, and the earthquake seismic displacement demand, derived from the inelastic response spectra. The ratio between the needed and the maximum available displacement d_u/d_p gives the structural safety level: if $d_u/d_p < 1$ the collapse occurs. Figure 12 shows this ratio as a function of the seismic level and the masonry properties. This 3D visualization also permits one to extrapolate the seismic behaviour for intermediate masonry properties, even if not directly considered. Moreover, these curves give important information for assessing the effectiveness of the possible strengthening techniques. In fact, once the structural safety level is defined, the designer can obtain the corresponding increase of the material strength, which is requested required in order to reach the target structural performance. Such an approach is typical in the field of the *Performance Based Design*.

8. Conclusions

In this paper, a practical methodology has been worked out in order to evaluate the seismic safety level of existing masonry arch bridges. Two particular case studies have been considered: a stone masonry bridge with brick-made vaults and a stone masonry bridge with concrete-made vaults. The structural analysis was carried out by making use of a simplified inelastic procedure: the structural capacity, obtained by a nonlinear static (*pushover*) analysis, was directly compared with the demand of the earthquake ground motion described by an inelastic response spectrum, in order to estimate the seismic performance of the bridges.

Such a method is particularly attractive because it permits one to consider explicitly the nonlinear structural behaviour and the fundamental role of the displacement, which is the real effect of the earthquake on the structure.

The choice of the control node in order to evaluate the reference displacement is, however, not unique and could produce some bias in the results. In the first part of the study, three different locations for the control node proposed in the literature were compared.

The common choice of the top elevation node does not seem appropriate, because it implies a more flexible structure and always leads to the highest estimate of the safety factor. The selection of the energy equivalent displacement, in contrast, appears more suitable because it leads to results on the safe side and is representative of the bridge's deformed shape near the collapse. A compromise choice is the centre of mass of the bridge, which is very near to the energy equivalent results but has a clearer geometrical interpretation and requires less computational effort.

Although available commercial software has actually many limitations, the methodology defined in the present work seems to be suitable for a careful seismic assessment of existing bridges without resorting to specialised packages. In particular, the seismic safety of the S. Marcello Pistoiese and Cutigliano Bridges was demonstrated by ascertaining that their displacement capacities are higher than the seismic demands of the sites in which they are located, for the whole range of the masonry material properties that bound the actual ones.

Acknowledgements

The authors gratefully acknowledge the financial support of MIUR–Cofin 2004081027_003. The authors also acknowledge the Pistoia County Administration, in the persons of Eng. Paolo Mazzoni and Eng. Paolo Bellezza. Finally, the authors wish to thank Linda Leprotti for her helpful collaboration.

References

[1] Heyman J. The masonry arch. Chichester: Ellis Horwood; 1982.

[2] Gilbert M, Melbourne C. Rigid-block analysis to masonry arches. *Structural Engineering* 1994; 72: 356–361.

[3] Hughes TG, Blackler MJ. A review of the UK masonry assessment methods. *Proceedings of the Institution of Civil Engineers* 1995; 110: 373–382.

[4] Boothby T. Collapse modes of masonry arch bridges. *Journal of the British Masonry Society* 1995; 9 (2): 62–69.

[5] Molins C, Roca P. Capacity of masonry arches and spatial frames. *J Struct Eng* 1988; 124: 653–663.

[6] Brencich A, De Francesco U. Assessment of multi-span masonry Arch bridges. Part I: a simplified approach, Part II: examples and applications. *J Bridge Eng ASCE* 2004; 9 (November): 582–598.

[7] Audenaert A., Fanning P., Sobczak L., Peremans H. 2-D analysis of arch bridges using an elasto-plastic material model. *Engineering Structures* 2008; 30: 845–855.

[8] Thavalingam A., Bicanic N., Robinson J. I., Ponniah D. A. Computational framework for discontinuous modelling of masonry arch bridges. *Computers and structures* 2001; 79: 1821-1830.

[9] Gilbert M. RING masonry arch analysis software. http://www.ring.shef.ac.uk/

[10] Cavicchi A, Gambarotta L. Collapse analysis of masonry bridges taking into account arch–fill interaction. *Engineering Structures* 2005; 27: 605–615.

[11] Cavicchi A, Gambarotta L. Lower bound limit analysis of masonry bridges including arch–fill interaction. *Engineering Structures* 2007; 29: 3002–3014.

[12] Fanning PJ, Boothby TE. Three-dimensional modelling and full-scale testing of stone arch bridges. *Journal of Computers and Structures* 2001; 79 (29–30):2645–2662.

[13] Fanning PJ, end Sobczak L, Boothby TE, Salomoni V. Load testing and model simulations for a stone arch bridge. *Bridge Structures* 2005; 1 (4).

[14] Resemini S. *Vulnerabilità sismica dei ponti ferroviari ad arco in muratura*. Tesi di Dottorato. XV Ciclo, Genova, 2003.

[15] UNI ENV 1998-1 (Eurocode 8). *Design of structures for earthquake resistance, Part 1: General rules, seismic actions and rules for buildings*. December 2003.

[16] Ordinanza P.C.M. 3274 *Primi elementi in materia di criteri generali per la classificazione sismica del territorio nazionale e di normative tecniche per le costruzioni in zona sismica* (in Italian). Release 9/9/2004.

[17] Ordinanza P.C.M. 3431. Ulteriori modifiche ed integrazioni alla Ordinanza PCM 3274 Primi Elementi in Materia di Criteri Generali per la Classificazione Sismica del Territorio Nazionale e di Normative Tecniche per le Costruzioni in Zona Sismica (in Italian). Release 3/5/2005.

[18] FEMA 440. *Improvement of Nonlinear Static Seismic Analysis Procedures*. Federal Emergency Management Agency, Washington, D.C., June 2005.

[19] FEMA 356. *Prestandard and Commentary for the seismic rehabilitation of buildings*. Federal Emergency Management Agency, Washington, D.C., November 2000.

[20] Gucci N., Barsotti R. A non-destructive technique for the determination of mortar load capacity in situ. *Materials and Structures* 1995; 28: 276 - 283.

[21] G+D Computing ©. Straus7 user’s manual (G+D Computing, Sidney Australia; HSH srl, Padova Italy) 1999.

[22] Brencich A., Sabia D. Experimental identification of a multi-span masonry bridge: The Tanaro Bridge. *Construction and Building Materials* 2008; 22: 2087–2099.

[23] Aprile A., Benedetti A., Grassucci F. Assessment of cracking and collapse for old brick masonry columns. *Journal of Structural Engineering* 2001; 127 (12): 1427-1435.

[24] Chen WF. *Plasticity in Reinforced Concrete*. Mc Graw-Hill Book Company: New York.

[25] Fajfar P. Structural Analysis in Earthquake Engineering – a breakthrough of Simplified Nonlinear Methods. *Proceeding of 12th European Conference on Earthquake Engineering*, 2002.

[26] Fajfar P. A Nonlinear Analysis Method for Performance-Based Seismic Design. *Earthquake Spectra* 2000; 16 (3): 573-592.

[27] Gupta B, Kunnath SK. Adaptive spectra-based pushover procedure for seismic evaluation of structures. *Earthquake Spectra* 2000; 16 (2); 367-392.

[28] Freeman SA, Nicoletti JP, Tyrrell JV. Evaluation of existing buildings for seismic risk – A case study of Puget Sound Naval Shipyard. *Proceeding of U.S. National Conference on Earthquake Engineering* 1975. Earthquake Engineering Research Inst., Oakland, California.

[29] Freeman SA. Development and use of capacity spectrum method. *Proceeding of Sixth U.S. National Conference on Earthquake Engineering* 1998, Earthquake Engineering Research Inst., Oakland, California.

[30] Vidic T, Fajfar P, Fischinger M. Consistent inelastic design spectra: strength and displacement. *Earthquake Engineering and Structural Dynamics* 1994; 23: 502-521.

[31] Lagomarsino S., Galasco A., Penna A. Pushover and dynamic analysis of U.R.M. buildings by means of a non-linear macro-element model. *Proceeding of the International Conference on Earthquake Loss Estimation and Risk Reduction*, Bucharest, 2002.

[32] Mwafy A.M., Elnashai A.S. Static pushover versus dynamic collapse analysis of RC buildings. *Engineering structures* 2001; 23: 407-424.

[33] Hernández-Montes E., Kwon O.-S., Aschheim M. An energy-based formulation for first and multiple-mode nonlinear static (pushover) analyses. *Journal of Earthquake Engineering* 2004; 8(1): 69–88.

[34] Tjhin T., Aschheim M., Hernández-Montes E. Estimates of Peak Roof Displacement Using “Equivalent” Single Degree of Freedom Systems. *Journal of Structural Engineering* 2005; 131 (3): 517-522.

[35] Martínez G., Roca P., Caselles O., Clapés J. Characterization of the Dynamic Response for the Structure of Mallorca Cathedral. *Proceeding of 5th International Conference on Structural Analysis of Historical Constructions*, New Delhi, India, 2006.

[36] Irizarry J., Podestà S., Resemini S. Capacity curves of monumental-heritage elements: the Santa Maria del Mar Church in Barcelona. *Proceeding of International Conference on Earthquake Loss Estimation and Risk Reduction*, Bucharest, 2002.

[37] Parducci A., Comodini F., Mezzi M. Approccio Energetico per le Analisi Pushover (in Italian). *XI National Congress "L'ingegneria Sismica in Italia"*, Genova, Italy, 2004.

[38] Parducci A., Comodini F., Lucarelli M., Mezzi M., Tomassoli E. Energy-Based Non Linear Static Analysis. *Proceeding of the First European Conference on Earthquake Engineering and Seismology,* Geneva, Switzerland, 2006.

Figures

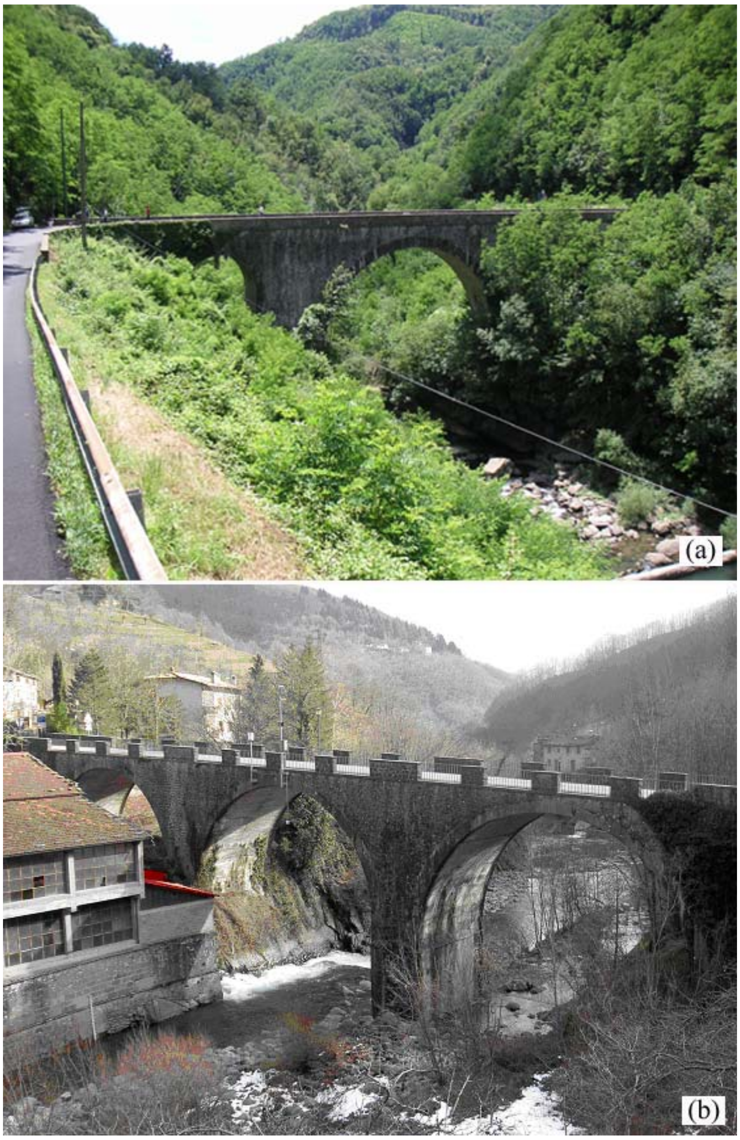

Fig. 1: *View of the two structures: a) S. Marcello Pistoiese Bridge; b) Cutigliano Bridge.*

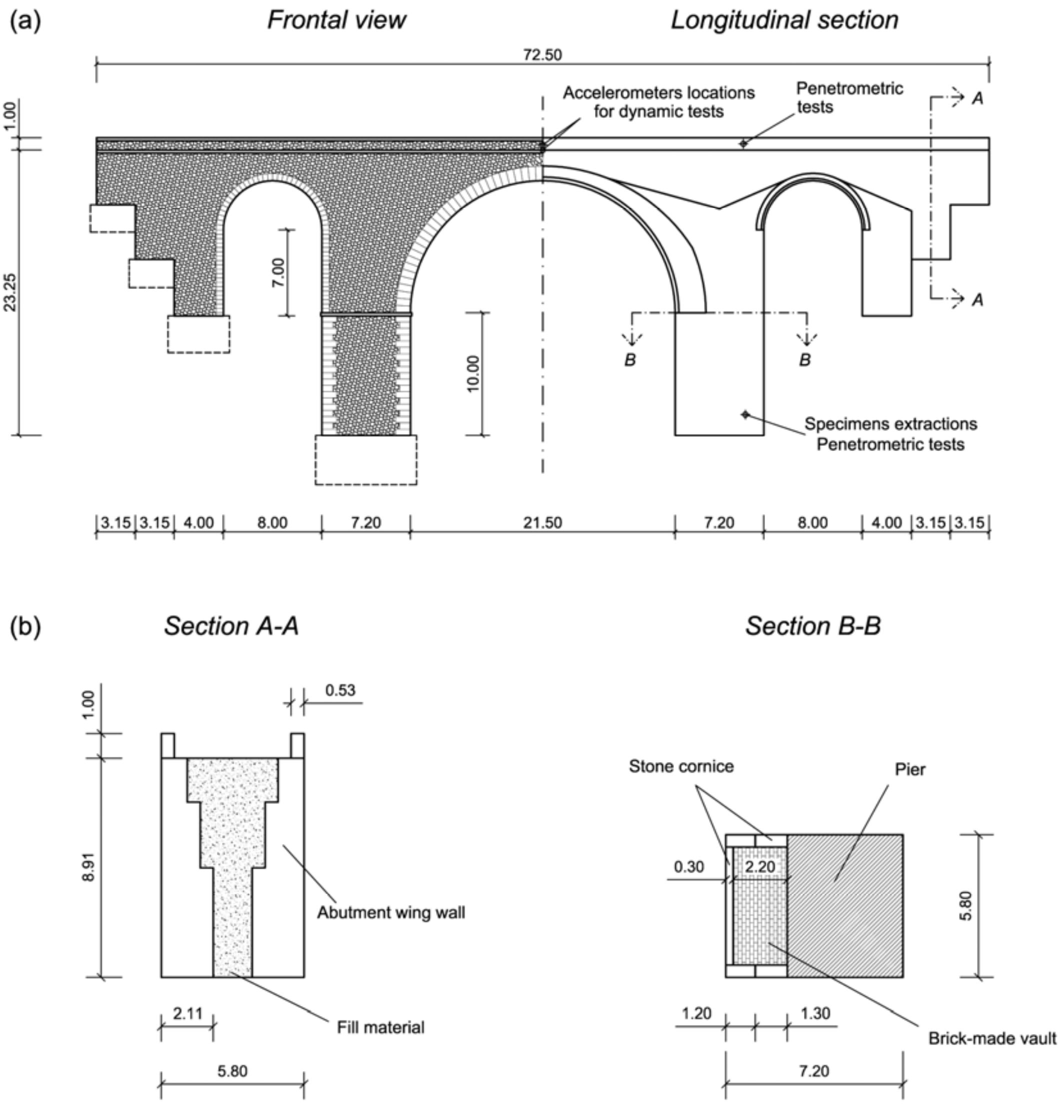

Fig. 2*: S. Marcello Pistoiese Bridge: (a) frontal view and longitudinal section; (b) transversal sections.*

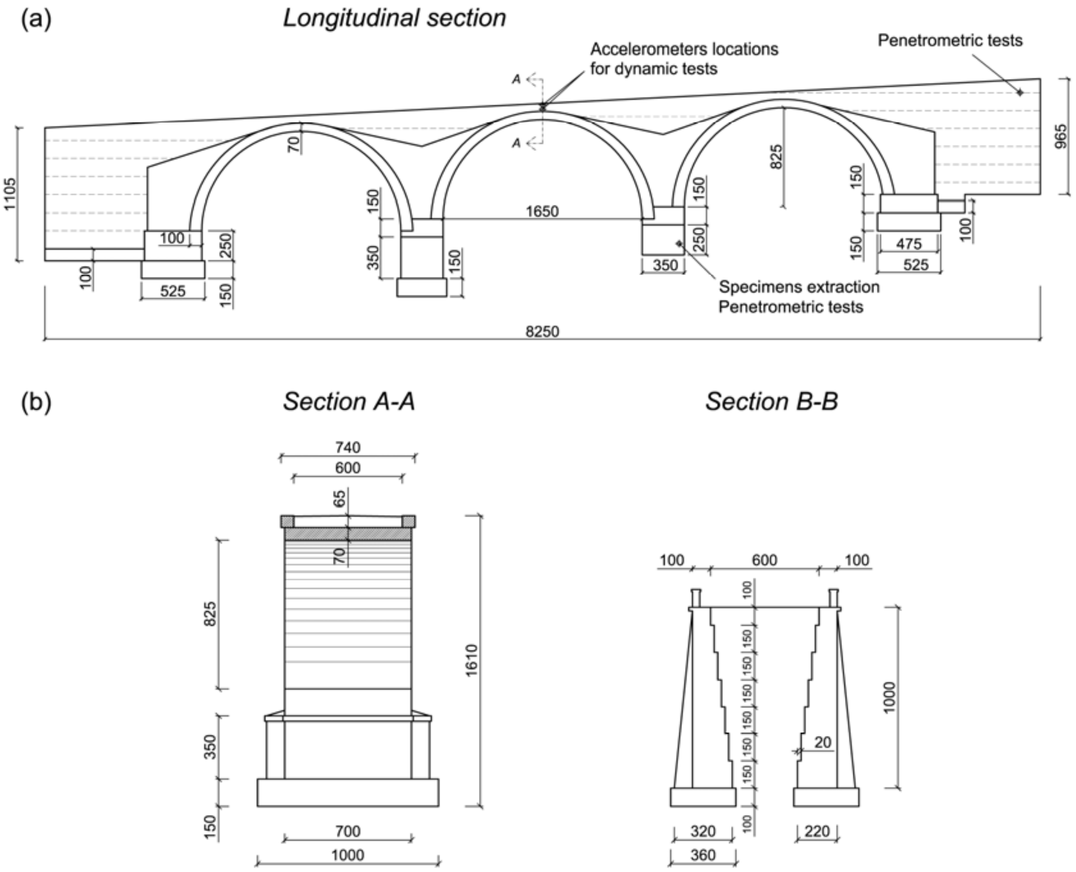

Fig. 3*: Cutigliano Bridge: (a) longitudinal section; (b) transversal sections.*

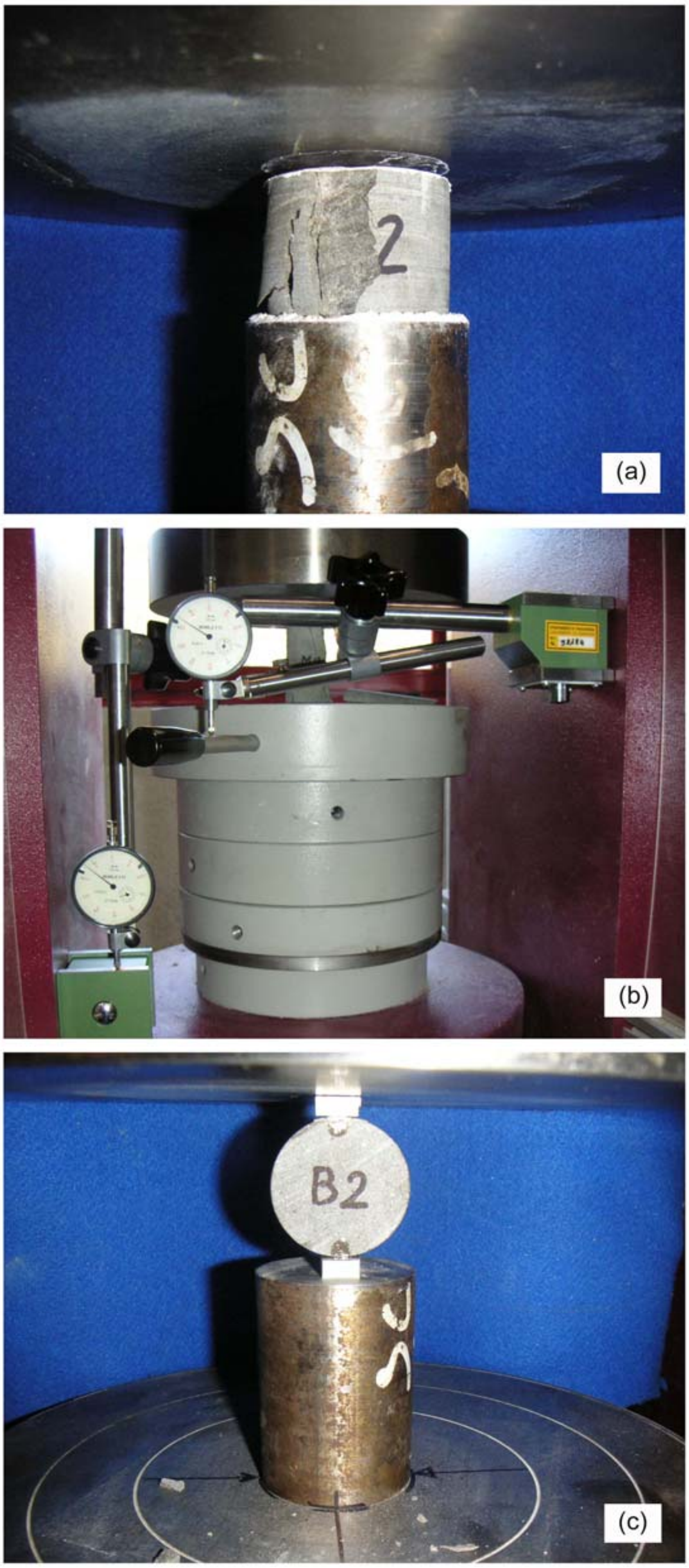

Fig. 4*: Laboratory tests: (a) compression test; (b) compression test with elastic modulus evaluation; (c) splitting test.*

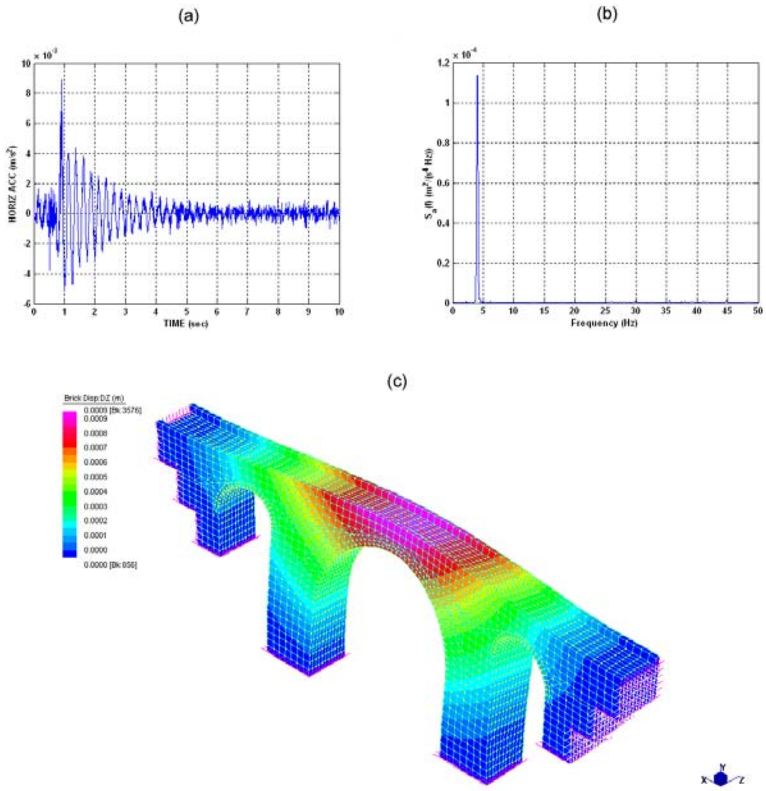

Fig. 5*: Dynamic on-site test of the S. Marcello Pistoiese bridge: (a) registered horizontal acceleration; (b) power spectral density of the dynamic response; (c) Mode n° 1 - Frequency = 3.998 Hz.*

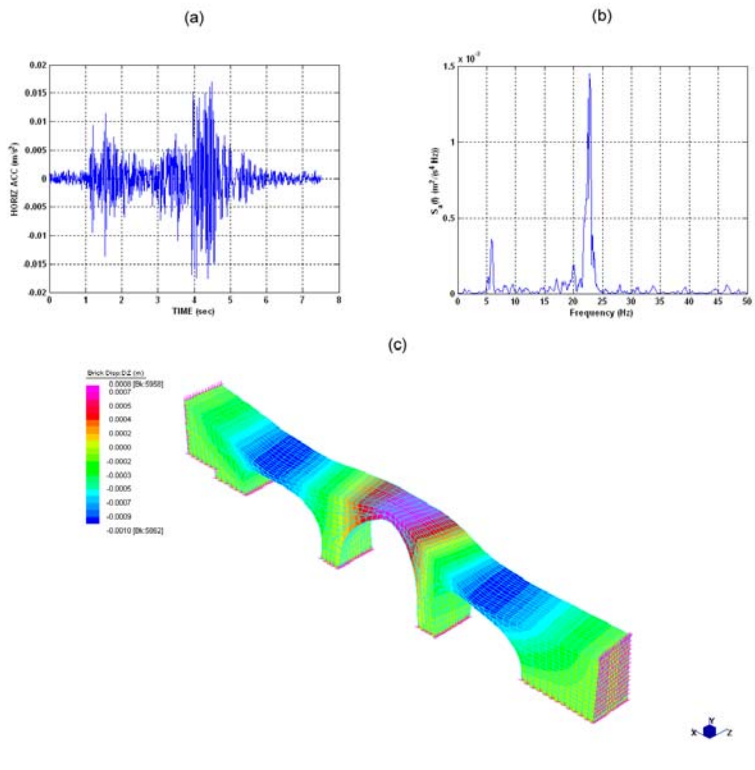

Fig. 6*: Dynamic on-site test of the Cutigliano bridge: (a) registered horizontal acceleration; (b) power spectral density of the dynamic response; (c) Mode n° 4 - Frequency = 23.1 Hz.*

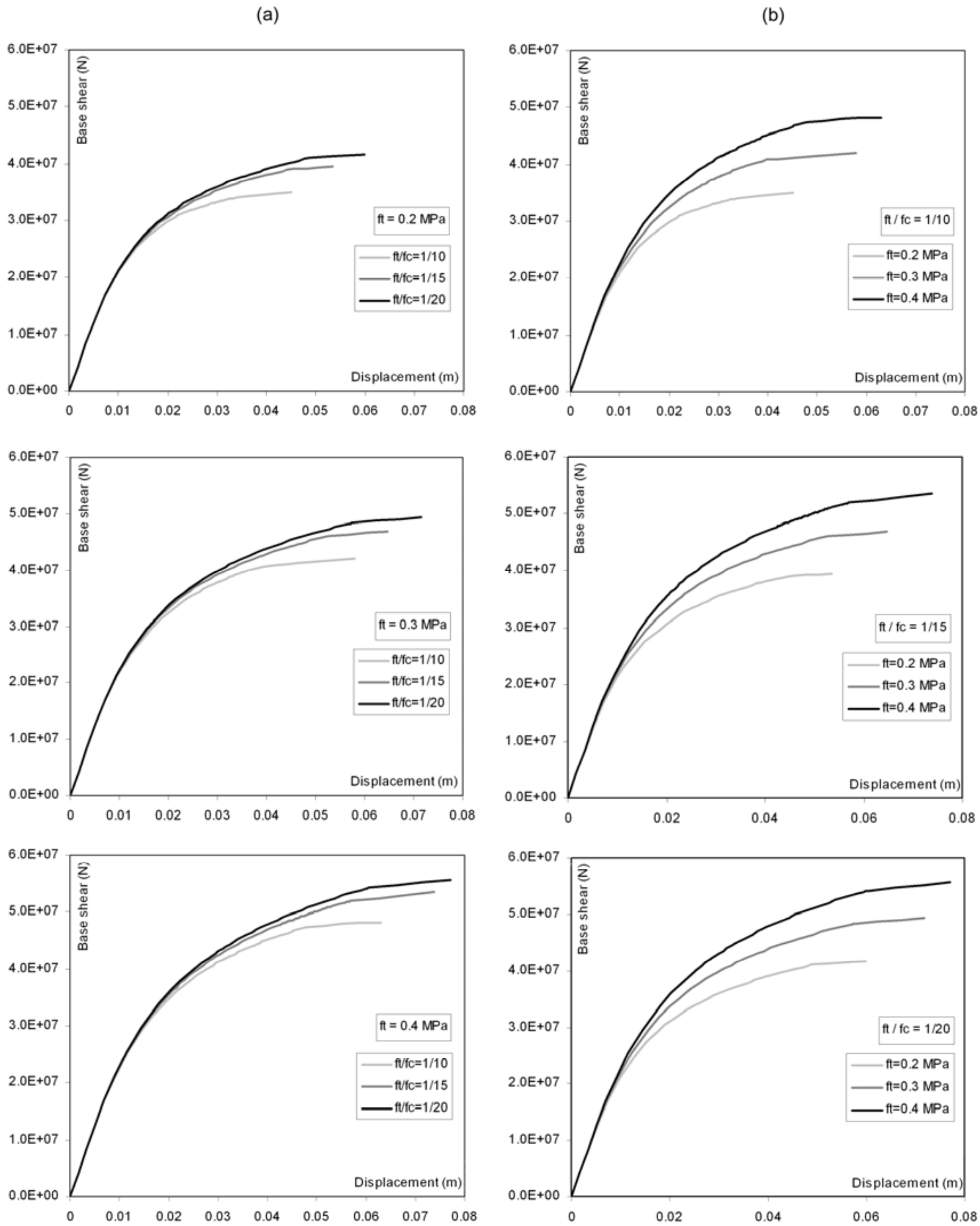

Fig. 7*: Pushover curves for the S. Marcello Pistoiese Bridge: (a) influence of the compressive strength* f_c *; (b) influence of the tensile strength* f_t *.*

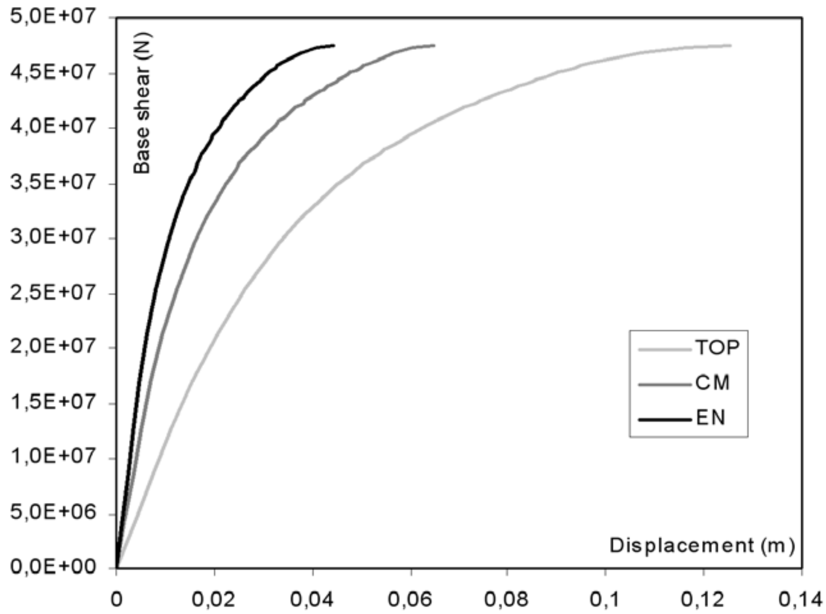

Fig. 8: *Pushover curves for the S. Marcello Pistoiese Bridge making reference to the top of the structure displacement (TOP), the centre of mass displacement (CM) and the virtual energy equivalent displacement (EN).*

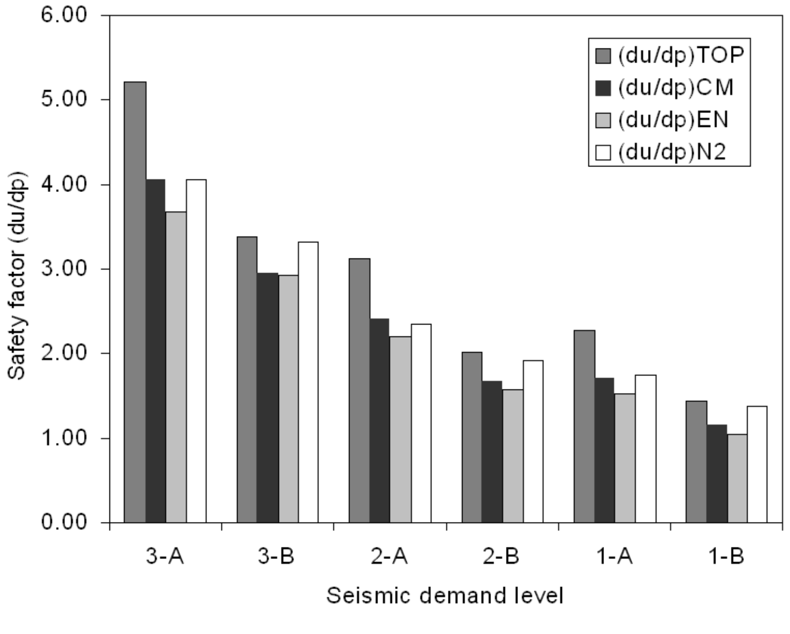

Fig. 9: *Comparison between the safety factors d_u/d_p determined considering the top displacement (TOP), the centre of mass displacement (CM), the virtual energy equivalent displacement (EN) and the N2 displacement (N2).*

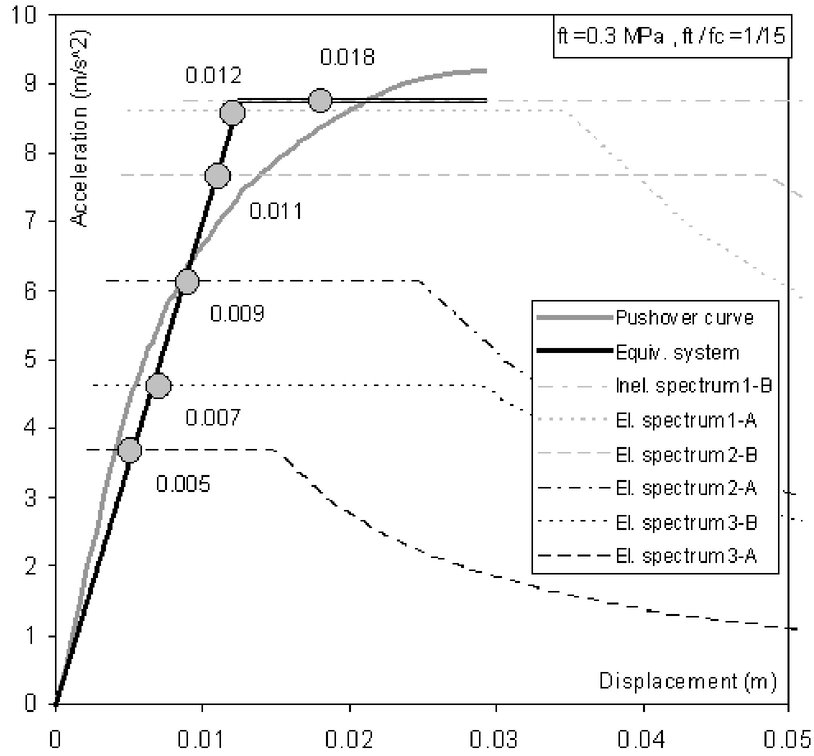

***Fig. 10**: Cutigliano Bridge performance points for different seismic levels and ground types (f_t =0.3 MPa , f_t/f_c =1/15).*

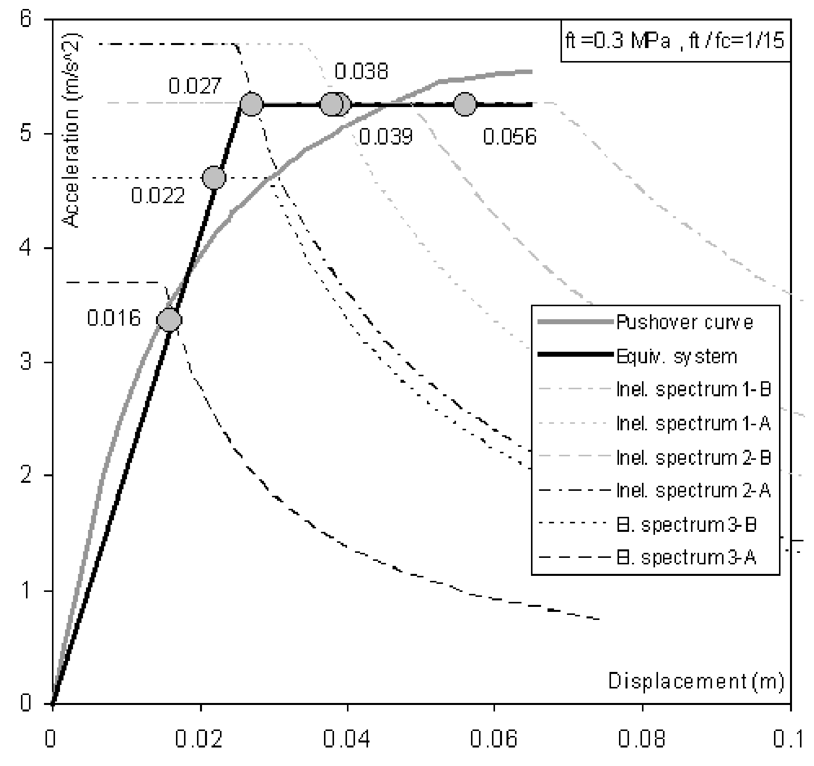

***Fig. 11**: S. Marcello Pistoiese Bridge performance points for different seismic levels and ground types (f_t =0.3 MPa , f_t/f_c =1/15).*

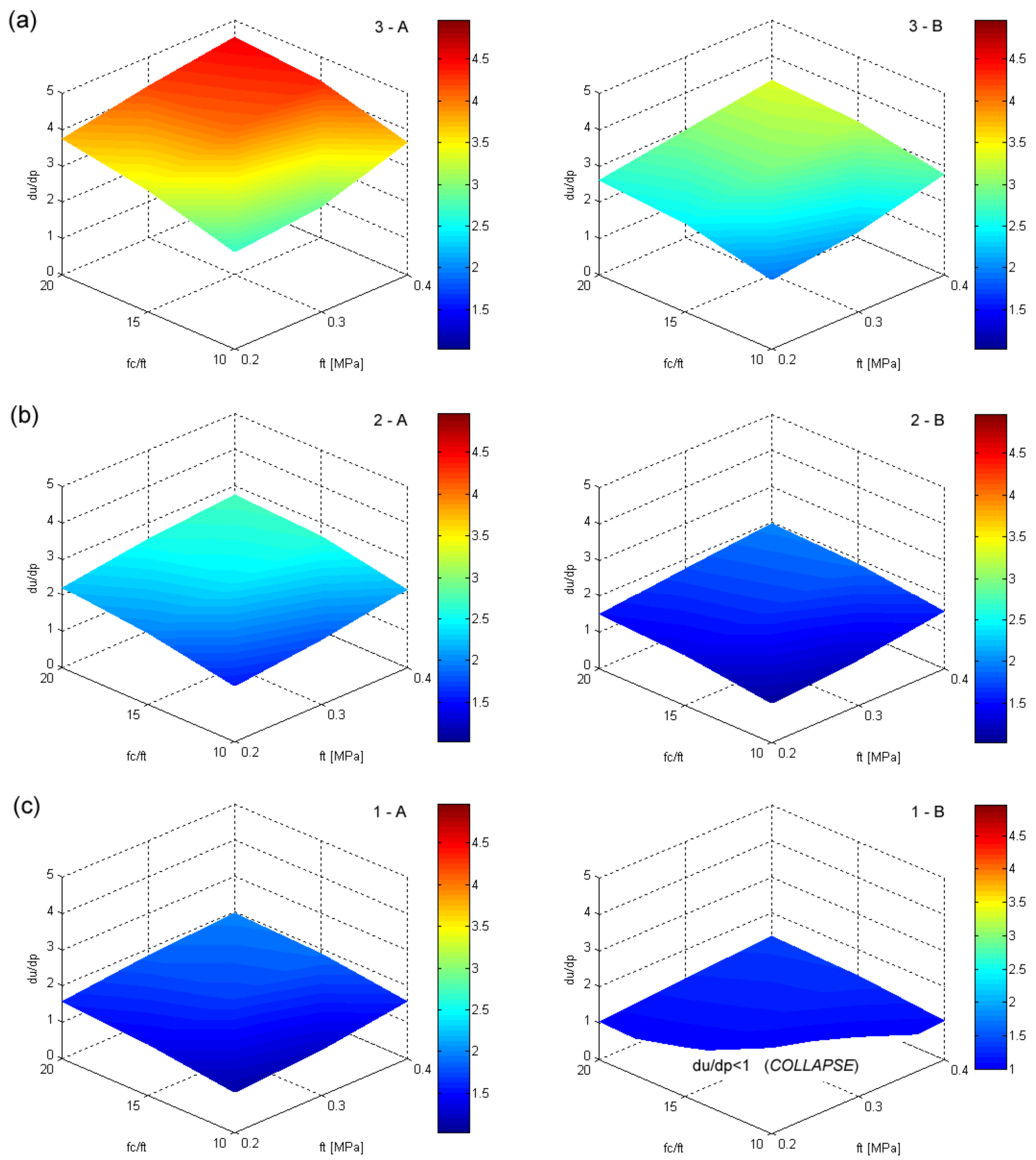

Fig. 12: *Ratios between the needed and the maximum available displacement d_u/d_p for different masonry properties of the S. Marcello Pistoiese bridge: (a) 3rd category seismic zone, ground type A vs. ground type B; (b) 2nd category seismic zone, ground type A vs. ground type B; (c) 1st category seismic zone, ground type A vs. ground type B.*

Tables captions

Tab. 1*: Geometrical data of the S. Marcello Pistoiese Bridge.*

S. MARCELLO PISTOIESE BRIDGE		
Total length		72.5 m
Width		5.80 m
Height over the mean water level		23.25 m
Parapets height		1.00 m
Arches number		3
PIERS		
Width		5.80 m
Length		7.20 m
Height		10.0 m
MAIN ARCH		
Span		21.5 m
Rise at midspan		10.75 m
Brick vault thickness	At the springing	2.20 m
	At the key	0.90 m
Stone cornice thickness		0.30 m
Total arch thickness	At the springing	2.50 m
	At the key	1.20 m
Depth of the fill at the crown		1.30 m
LATERAL ARCHES		
Span		8.00 m
Rise at midspan		4.00 m
Brick vault thickness		0.40 m
Stone cornice thickness		0.20 m
Total arch thickness		0.60 m
Depth of the fill at the crown		1.90 m

Tab. 2*: Geometrical data of the Cutigliano Bridge.*

CUTIGLIANO BRIDGE		
Total length		82.5 m
Width		7.40 m
Height over the mean water level		16 m
Deck gradient		5%
Arches number		3
PIERS		
Width		3.50 m
Length		7.00 m
Height	Upper pier	3.50 m
	Lower pier	2.50 m
DOSSERETS ABOVE THE PIERS		
Width		3.50 m
Length		7.00 m
Height		1.50 m
STRUCTURAL ARCHES		
Span		16.50 m
Rise at midspan		8.25 m
Concrete vault thickness	At the springing	1.00 m
	At the key	0.70 m
Depth of the fill at the crown		0.65 m

***Tab. 3**: Laboratory tests results on stone specimens: compression test; compression test with elastic modulus evaluation; splitting test.*

Mechanical characteristic	Specimen	Test result
Compressive strength	C1	100.3 MPa
	C2	52.0 MPa
	C3	44.9 MPa
	M1	86.0 MPa
Elastic modulus	M1	14528 MPa
Tensile strength	B1	13.2 MPa
	B2	15.6 MPa
	B3	14.6 MPa

***Tab. 4**: Structural parameters adopted in the numerical models of the bridges: material density (γ), Young Modulus (E) and Poisson ratio (v).*

Bridge	Material	γ (kg/m^3)	E (MPa)	ν (-)
S. MARCELLO PISTOIESE	Masonry of stone and lime mortar (*piers, spandrel walls, abutments , parapets)*	2200	5000	0.2
	Masonry of stone and concrete mortar (*arch cornice*)	2200	6000	0.2
	Masonry of bricks and concrete mortar (*vaults*)	1800	5000	0.2
	Backfill	1800	500	0.2
CUTIGLIANO	Masonry of stone and lime mortar (*piers, spandrel walls, abutments , parapets)*	2200	5000	0.2
	Concrete (*dosserets and vaults)*	2400	12000	0.2
	Backfill	1800	500	0.2

***Tab. 5**: Drucker-Prager's parameters ϕ and c for stone masonry corresponding to the considered values of the uniaxial tensile strength f_t and the compressive strength f_c of the homogenized continuum* [24].

Tensile strength f_t (MPa)	Strengths ratio f_t/f_c (-)	Compressive strength f_c (MPa)	Friction angle ϕ (deg)	Cohesion c (MPa)
0.2	1/10	2	55°	0.32
	1/15	3	61°	0.39
	1/20	4	65°	0.45
0.3	1/10	3	55°	0.47
	1/15	4.5	61°	0.58
	1/20	6	65°	0.67
0.4	1/10	4	55°	0.63
	1/15	6	61°	0.77
	1/20	8	65°	0.89

Tab. 6: *Performance displacements (d_p) and safety factors (d_u/d_p) obtained for the different control node positions: top, centre of mass, energy-equivalent, N2 method.*

Spectrum	PERFORMANCE POINT				SAFETY FACTOR					
	$d_{p,TOP}$ (m)	$d_{p,CM}$ (m)	$d_{p,EN}$ (m)	$d_{p,N2}$ (m)	$(d_u/d_p)_{TOP}$ (-)	$(d_u/d_p)_{CM}$ (-)	$(d_u/d_p)_{EN}$ (-)	$(d_u/d_p)_{N2}$ (-)	Mean (-)	C.O.V. (%)
3-A	0.024	0.016	0.012	0.018	5.21	4.06	3.67	4.06	4.25	13.6
3-B	0.037	0.022	0.015	0.022	3.38	2.95	2.93	3.32	3.15	6.5
2-A	0.040	0.027	0.020	0.031	3.13	2.41	2.20	2.35	2.52	14.1
2-B	0.062	0.039	0.028	0.038	2.02	1.67	1.57	1.92	1.79	10.1
1-A	0.055	0.038	0.029	0.042	2.27	1.71	1.52	1.74	1.81	15.5
1-B	0.087	0.056	0.042	0.053	1.44	1.16	1.05	1.38	1.26	12.6

Tab. 7: *S. Marcello Pistoiese Bridge ultimate displacements, performance points and safety factors for different seismic demands and masonry properties.*

ft	ft/fc	Soil type	ULTIMATE DISPLACEMENT	PERFORMANCE POINT (m)			SAFETY FACTOR		
				Spectrum type			Spectrum type		
(MPa)	(-)		(m)	3	2	1	3	2	1
0.2	1 / 10	A	0.040	0.015	0.026	0.036	2.67	1.54	1.11
0.2	1 / 15		0.054	0.016	0.027	0.038	3.35	1.98	1.41
0.2	1 / 20		0.060	0.016	0.027	0.038	3.75	2.22	1.58
0.3	1 / 10		0.046	0.016	0.026	0.037	2.90	1.79	1.25
0.3	1 / 15		0.065	0.016	0.027	0.038	4.04	2.39	1.70
0.3	1 / 20		0.072	0.017	0.028	0.039	4.21	2.56	1.84
0.4	1 / 10		0.059	0.016	0.027	0.037	3.66	2.17	1.58
0.4	1 / 15		0.074	0.017	0.028	0.039	4.34	2.64	1.89
0.4	1 / 20		0.077	0.017	0.028	0.039	4.53	2.75	1.98
0.2	1 / 10	B	0.040	0.021	0.037	0.053	1.91	1.08	COLLAPSE
0.2	1 / 15		0.054	0.022	0.039	0.055	2.44	1.37	COLLAPSE
0.2	1 / 20		0.060	0.023	0.040	0.057	2.61	1.50	1.05
0.3	1 / 10		0.046	0.021	0.037	0.053	2.21	1.25	COLLAPSE
0.3	1 / 15		0.065	0.022	0.039	0.056	2.94	1.66	1.15
0.3	1 / 20		0.072	0.024	0.041	0.058	2.98	1.75	1.24
0.4	1 / 10		0.059	0.021	0.037	0.054	2.79	1.58	1.08
0.4	1 / 15		0.074	0.023	0.039	0.056	3.21	1.89	1.32
0.4	1 / 20		0.077	0.023	0.039	0.056	3.35	1.98	1.38